Alkane Bromination Revisited: "Reproportionation" in Gas-Phase Methane Bromination Leads to Higher Selectivity for CH_3Br at Moderate Temperatures

Ivan M. Lorkovic,*,† Shouli Sun,‡ Sagar Gadewar,‡ Ashley Breed,‡ Gerald S. Macala,† Amin Sardar,‡ Sarah E. Cross,† Jeffrey H. Sherman,‡ Galen D. Stucky,† and Peter C. Ford†

Department of Chemistry and Biochemistry, University of California, Santa Barbara, Santa Barbara, California 93103, and Gas Reaction Technologies, 861 Ward Drive, Santa Barbara, California 93111

Received: March 14, 2006; In Final Form: April 26, 2006

The reaction of methane and bromine is a mildly exothermic and exergonic example of free radical alkane activation. We show here that the reaction of methane and bromine (CH_4:$Br_2 \geq 1$) may yield either a kinetically or a thermodynamically determined bromomethane product distribution and proceeds in two main phases between 450 and 550 °C under ambient pressure on the laboratory time scale. This is in contrast to the highly exothermic methane fluorination or chlorination reactions, which give kinetic product distributions, and to the endergonic iodination of methane, which yields an equilibrium distribution of iodomethanes. The first phase of reaction between methane and bromine is a relatively rapid consumption of bromine to yield a kinetic methane bromination product distribution characterized by low methane conversion, low methyl bromide selectivity, and higher polybromomethane selectivity. In the second slower phase CH_xBr_{4-x} reproportionation leads to significantly higher methane conversion and higher methyl bromide selectivity. For methane bromination at 525 °C, CH_4 conversion and CH_3Br selectivity reach 73.5% and 69.5%, respectively, after ample (60 s) time for reproportionation. The high selectivity and simple configuration make this pathway an attractive candidate for scale-up in halogen-mediated methane partial oxidation processes.

Introduction

Methane activation by free radical initiation is one of the most extensively studied methane functionalization pathways. These reactions have importance in the chemical industry and in understanding and controlling combustion, as well as in atmospheric chemistry. Among the radicals commonly used to initiate such reactions, halogens stand out as being the best understood (eq 1):

$$CH_4 + X_2 \rightarrow CH_3X + HX \quad (1a)$$

$$CH_4 + 2X_2 \rightarrow CH_2X_2 + 2HX \quad (1b)$$

$$CH_4 + 3X_2 \rightarrow CHX_3 + 3HX \quad (1c)$$

$$CH_4 + 4X_2 \rightarrow CX_4 + 4HX \quad (1d)$$

Most literature on methane halogenation describes measurements of fundamental constants associated with these reactions such as bond strengths (C−H, C−Br, etc.), rate constants, and other fundamental parameters.[1−6] Relatively little work has focused on determining product distributions of reactions between methane and halogens under a given set of conditions with emphasis on maximizing desirable product yield.

In the context of our program to develop partial oxidation chemistry using solid metal bromides/oxides as mediators via bromine production and recovery,[7−14] we have performed extensive studies in light alkane bromination, with the aim of developing an efficient and selective catalyst for methane monobromination. In the course of these studies it became apparent that the highest yields of methyl bromide were obtained when would-be catalysts were altogether absent, that is, when the reactor was an empty hot tube. We were further surprised to find that the highest methyl bromide selectivities were obtained under conditions that we expected, through side reactions, would lead to the poorest selectivities, namely, high temperature and long reaction time.

We report here our findings in greater detail, and we reach the conclusion that gas-phase methane bromination occurs in two phases, the first coinciding with bromine consumption and leading to a kinetic distribution of poor CH_3Br selectivity, and the second slower phase associated with CH_xBr_{4-x} reproportionation and yielding superior CH_3Br selectivity. Thus methane bromination product distributions, in contrast to those of methane chlorination and iodination, are tunable within quite broad bounds determined by kinetic and quasithermodynamic (for an equilibrium constrained to C_1 species) limits. CH_3Br, CH_2Br_2, and $CHBr_3$ selectivities may be controlled by altering temperatures of reaction over a range between 350 and 550 °C or by altering reaction times at a given temperature. This two-stage behavior is in fact predicted by the bond strengths and activation barriers involved in the fundamental steps leading to the observed distribution.[15] However, the observed equilibrated bromocarbon distribution differs significantly from the "thermodynamic" distribution calculated from available thermodynamic data.[16,17] Therefore, these measurements may serve to refine available experimental thermodynamic data for (poly)-

† University of California, Santa Barbara.
‡ Gas Reaction Technologies.

10.1021/jp061558h CCC: $33.50
Published on Web 06/16/2006

SCHEME 1: Reactor Schematic for Methane Bromination Experiments

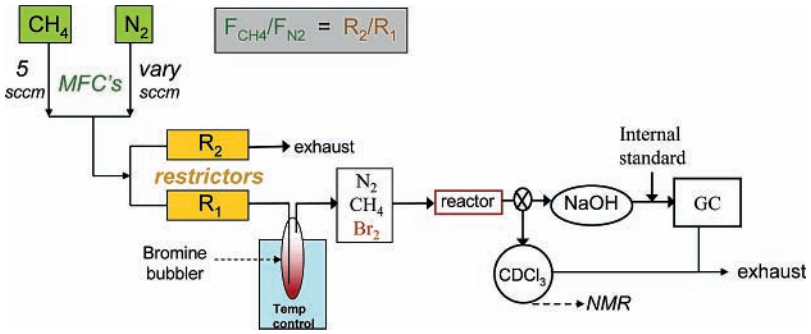

bromomethane thermodynamic constants. To our knowledge, CH_xBr_{4-x} reproportionation of a brominated methane stream leading to CH_3Br enrichment in the absence of catalyst has not been previously reported.

Experimental Section

Methane (Praxair, 3.7 grade), nitrogen (liquid N_2 boil-off, Praxair), and dimethyl ether (Aldrich) were delivered to the flow system, Scheme 1, through Matheson mass flow controllers. Only poly(tetrafluoroethylene) (PTFE) poly(chlorotrifluoroethylene) (CTFE), and Pyrex came into contact with bromine-containing streams. Bromine was delivered to the gas stream by means of a temperature-controlled (21 ± 1 °C) Pyrex bubbler. For high methane conversion experiments, methane was diluted with appropriate N_2 flow upstream from the bromine bubbler so that addition of bromine [$P(Br_2, 21\ °C) = 150$ Torr] gave a 1:1 methane to bromine mixture. The inner diameter of the PTFE plumbing was <1 mm for these atmospheric experiments, and so it was assumed that the gaseous mixture was well mixed prior to entering the heated reaction zone. The methane/N_2/bromine stream was then passed through a vertical tubular Pyrex reactor within a temperature-controlled aluminum block. For variable residence time experiments the heated volume was altered by varying tube diameter between 10 and 4 mm and also through use of a Pyrex tube with 1 mm inner diameter for short (<1 s) space time experiments. For all experiments, the heated volume aspect ratio was greater than 20.

Products exiting the reactor were further diluted with N_2, passed through a base trap (10 cm^3 of 2 M NaOH, 20 °C) to remove HBr, diluted with N_2 again, mixed with a dimethyl ether internal standard stream, and finally directed to a GC (HP6890, Restek Rt-QPLOT 30 m × 0.32 mm column) sampling loop for injection and analysis. Because of the dead volume effects of the base trap and of nonheated plumbing, integrations of multiple stream injections were performed even after bypass (shutoff) of the upstream bromine bubbler so that any polybromomethane lingering in the traps might be accounted for. Temperature was variable in our apparatus up to 550 °C, just below the melting point of the aluminum reactors and the temperature at which Pyrex begins to soften.

Reaction products were also quantified by ^1H Fourier transform (FT) NMR (delay time = 20 s between pulses), with a $CDCl_3$ (6 g collected for 30 min) trap with known [$CHCl_3$] as an integration standard to collect and quantify product. To eliminate plumbing holdup of semivolatiles upstream of the $CDCl_3$ trap, the bromine flow was initiated through the apparatus 3 h before attachment of the $CDCl_3$ trap just downstream of the reactor outlet. To account for any undissolved CH_3Br, a second identical trap was placed just downstream of the first.

Extent of reaction (ξ) measurements were performed in an empty tube reactor (10 cm^3) at variable temperature, with a methane carrier flow rate of 5 sccm. Methane was bubbled through CH_2Br_2 (40 Torr) and $CHBr_3$ (7 Torr) bubblers at room temperature and through $CHCl_3$ and Br_2 (~70 Torr) at 0 °C. Chlorine was introduced by N_2 purge (1.0 sccm) of a 1 L flask into which household bleach (100 cm^3, 5% chlorine) and HCl (50 cm^3, 20%) had been added (caution, this step requires impeccable ventilation). After an initial fast evolution of Cl_2, sustained Cl_2 delivery was achieved for the duration of the experiment.

Because methane conversion for these experiments is low and therefore difficult to measure, ξ was approximated for methane reaction with bromine and chlorine, as $1 - ([X_2]/[X_2]_0)$, where $[X_2]$ and $[X_2]_0$ are the halogen concentrations exiting the reactor in the presence and absence of reaction with methane. $[X_2]$ was measured by trapping unreacted halogen in the stream in caustic (10 cm^3 of 2 M NaOH, 20 °C) for a set time and determining $[OX^-]$ spectrophotometrically [301 $M^{-1}\ cm^{-1}$ (330 nm) and 350 $M^{-1}\ cm^{-1}$ (290 nm) for hypobromite and hypochlorite, respectively]. For the reaction between methane with CH_2Br_2, ξ was defined as $^1/_2CH_3Br/(^1/_2CH_3Br + CH_2Br_2)$; for reaction of methane with $CHBr_3$, as $^1/_2(CH_2Br_2 + CH_3Br)/(CHBr_3 + {}^1/_2CH_2Br_2 + {}^1/_2CH_3Br)$; and for the reaction of methane with $CHCl_3$, as $^1/_2(CH_3Cl + CH_2Cl_2)/(CHCl_3(0))$. ξ for reaction of $CHCl_3$ with methane is defined differently than for $CHBr_3$ because, while C_1 reproportionation leading to CH_3Cl and CH_2Cl_2 was still measurable, $CHCl_3$ decomposition (~50% at the highest temperature) was the dominant pathway observed. Reaction of methane with CH_2Cl_2 (entrained at −40 °C by use of an acetonitrile/CO_2 slush bath) showed only CH_2Cl_2 decomposition and gave no reproportionation products at temperatures up to 550 °C with a CH_4 flow of 5 sccm.

Results and Discussion

For thermal reactions of stoichiometric or substoichiometric bromine with methane, the bromomethane product distribution evolves in two main phases at temperatures high enough to observe full consumption of bromine on laboratory time scales (Figures 1 and 2). We propose that the two phases are best described as bromine consumption by methane and bromomethanes, eqs 2−10, followed by reproportionation of the CH_xBr_{4-x} products, which requires initiation by eqs 11−14 and propagation by eqs 15−35 in Appendix 1.

Fast Initiation

$$Br_2 \leftrightarrow 2Br \text{ (initiation 1)} \qquad (2)$$

$$Br + CH_4 \leftrightarrow HBr + CH_3 \text{ (initiation 2)} \qquad (3)$$

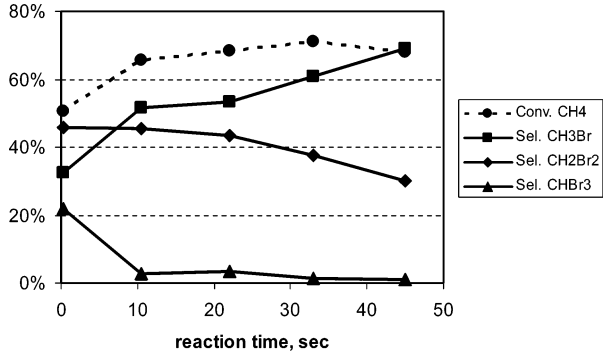

Figure 1. Reaction time dependence of the product distribution for the reaction $CH_4 + Br_2 \rightarrow A(x)\ CH_xBr_{4-x} + HBr$, 500 °C, 1 atm. These data differ significantly from the predicted values at 500 °C: CH_4 conversion, 59.6%; CH_3Br, CH_2Br_2, and $CHBr_3$ selectivity, 39.3%, 54.1%, and 6.5%.

Bromine Atom Propagations

$$CH_3 + Br_2 \rightarrow CH_3Br + Br \text{ (propagation)} \quad (4)$$

$$CH_3Br + Br \leftrightarrow CH_2Br + HBr \quad (5)$$

$$CH_2Br + Br_2 \rightarrow CH_2Br_2 + Br \quad (6)$$

$$CH_2Br_2 + Br \leftrightarrow CHBr_2 + HBr \quad (7)$$

$$CHBr_2 + Br_2 \rightarrow CHBr_3 + Br \quad (8)$$

$$CHBr_3 + Br \leftrightarrow CBr_3 + HBr \quad (9)$$

$$CBr_3 + Br_2 \rightarrow CBr_4 + Br \quad (10)$$

Slow Initiations

$$CBr_4 \leftrightarrow CBr_3 + Br \quad (11)$$

$$CHBr_3 \leftrightarrow CHBr_2 + Br \quad (12)$$

$$CH_2Br_2 \leftrightarrow CH_2Br + Br \quad (13)$$

$$CH_3Br \leftrightarrow CH_3 + Br \quad (14)$$

At 500 °C, the two phases are separated in time scale by approximately 2 orders of magnitude; bromine consumption occurs in ~0.5 s, while reproportionation occurs over ~100 s. In the first phase, methane conversion is relatively low, and the mixture of bromomethanes is relatively rich in CH_2Br_2 and $CHBr_3$. The second slower phase leads to higher methane conversion and more CH_3Br. Correspondingly, CH_2Br_2 yield drops by approximately a factor of 2, while $CHBr_3$ drops below 1%. If reaction temperature is varied instead of reaction time, similar two-phase behavior is observed, with the first phase of reaction occurring at 350−400 °C (60 s reaction time) and the second phase observable at 500−550 °C (60 s). As shown in Figure 2, changes in observed selectivity are at least an order of magnitude greater than the predicted temperature effects on the equilibrium between these species.

If during the first nonselective phase of methane bromination there is significant buildup of $CHBr_3$, or to a lesser extent CBr_4, the onset of bromine redistribution from these species to methane is faster and happens at lower temperature than the corresponding reaction for CH_2Br_2, and thus the second phase of bromine reproportionation is best described, perhaps pedantically, as consisting of two subphases corresponding to $CHBr_3$ and CH_2Br_2 activation of methane. This behavior can be seen in Figures 1 and 2; significant concentrations of $CHBr_3$ are present only at short reaction times at 500 °C and only at lower temperatures with a 1 min reaction time, while CH_2Br_2 concentrations drop less sharply at longer residence times and higher temperatures, consistent with a lower activation barrier for $CHBr_3$ reproportionation.

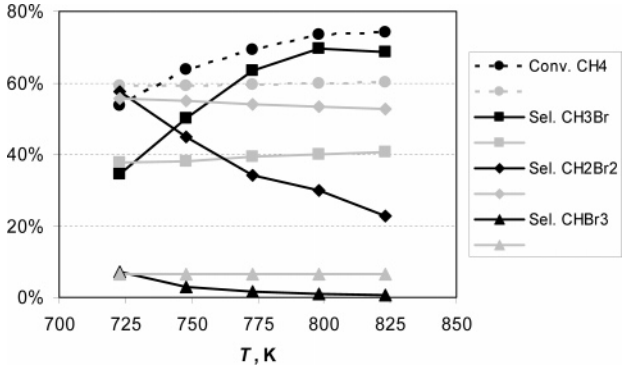

Figure 2. Predicted (gray) and observed (black) reaction temperature dependence of the product distribution for the reaction $CH_4 + Br_2 \rightarrow A(x)\ CH_xBr_{4-x} + HBr$, $\tau = 60$ s, 1 atm. The data at lower temperatures are best represented as kinetic distributions, while the higher temperature data are best represented as thermodynamic C_1 distributions. At 525 °C, the observed (predicted) conversion was 73.5% (59.6%), and selectivities for CH_3Br, CH_2Br_2, and $CHBr_3$, respectively, were 69.5% (39.3%), 29.5% (54.1%), and 1.0% (6.5%).

TABLE 1: Relevant Bond Dissociation Energies: Comparison between Cl, Br, and I[a]

	bond dissociation energy (kcal/mol)		
bond	X = Cl	X = Br	X = I
H−CH_3	105	105	105
H−X	103	88	71
H−CH_2X	100	102	100
H−CHX_2	97	99	93
H−CX_3	94	95	85
X−*CH*$_3$	*84*	*70*	*56*
X−*CH*$_2$*X*	*80*	*67*	*50*
X−*CHX*$_2$	*75*	*63*	*41*
X−*CX*$_3$	*70*	*56*	*29*
X−X	58	46	36

[a] Data were taken from refs 15,18, and 19 for all halomethanes and from refs 16 and 17 for CH_4, HX, and X_2.

TABLE 2: Enthalpy Barriers to Halogenations and Reproportionations[a]

	enthalpy barrier (kcal/mol)		
	X = Cl	X = Br	X = I
	Halogenation		
CH_4	60	64	70
CH_3X	58	61	65
CH_2X_2	58	57	
	Reproportionation		
CHX_3	83	69	
CH_2X_2	85 (25)	70 (6)	55 (−15)

[a] From data from Table 1. The difference between halogenation and reproportionation barriers is shown in parentheses. This information is shown pictorally in Scheme 2. The barriers for these reactions are calculated with the assumption of only dissociative free radical pathways for halogen exchange, for which no added barriers exist other than the energy required to create the radical intermediates by any path.

SCHEME 2: Methane Halogenation versus Halomethane Reproportionation Energetics

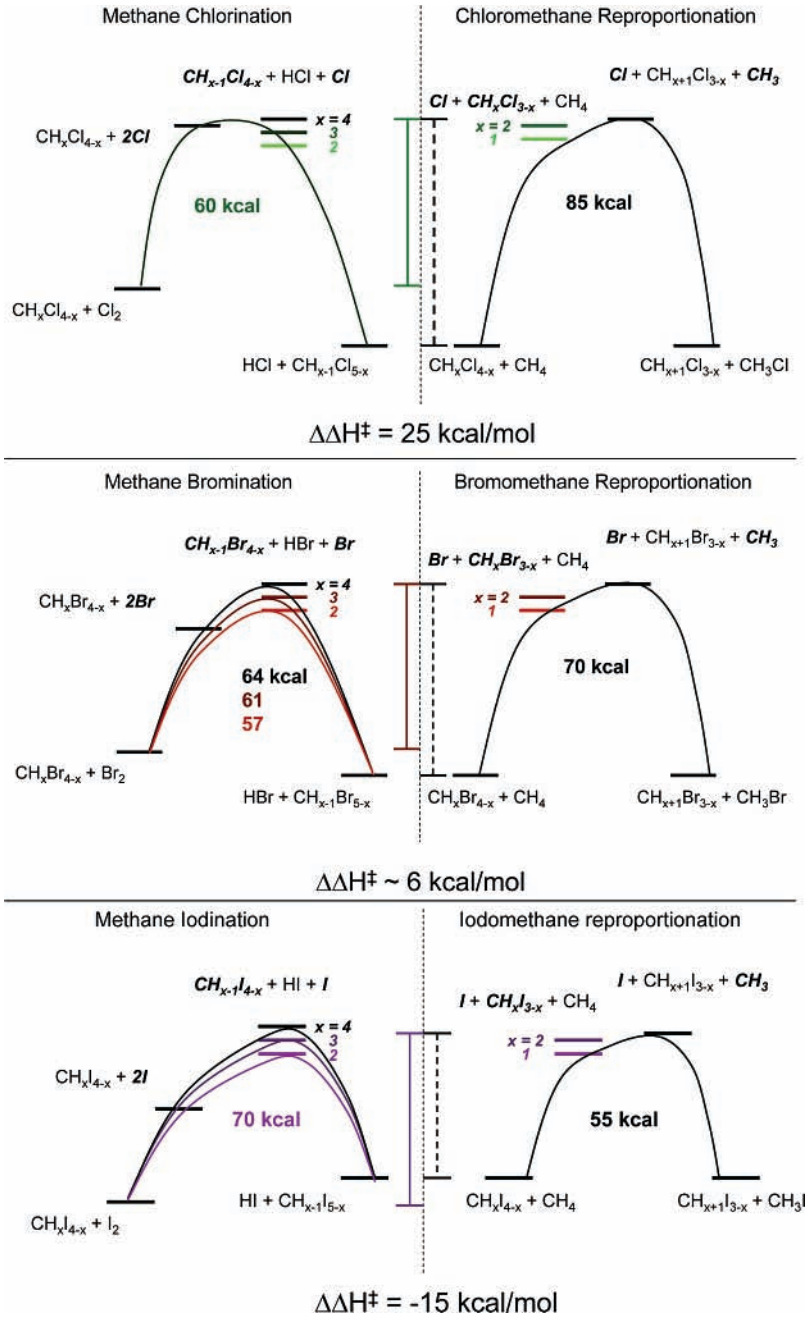

To attempt to elucidate this complex evolution of product distribution for an apparently simple reaction, it is instructive to compare and contrast these observations with predictions derived from bond strength estimates,[15] including similar predictions for methane chlorination[18] and methane iodination.[19] Table 1 shows the relevant bond strengths for all of the C_1 halomethanes of Cl, Br, and I. Using these bond strengths, one may develop an energy diagram (Scheme 2), showing the barrier heights for initiation and propagation reactions for methane halogenation and for halogen redistribution reactions. These values are listed in Table 2.

From the scheme it can be seen that the barrier for (chloro)-methane chlorination is almost entirely determined by the Cl_2 homolysis barrier, which is ~25 kcal/mol lower than the energy required for chloromethane homolysis, the necessary first step for chlorocarbon reproportionation. Thus, methane chlorination gives a kinetically determined product distribution, characterized by similar rates of reaction for primary and secondary methane chlorination over a wide temperature range and reaction time. For methane iodination, the opposite is true. The reproportionation reactions enjoy lower barriers than the initial primary iodination of methane, which is the slowest of all the steps in the scheme. Although the reaction is significantly uphill and the extent of reaction is low, the iodomethane product distribution at no time represents anything but an equilibrium C_1 mixture.

We obtained further support for our explanation of the reactions responsible for the marked shift in bromomethane selectivity at short and long time scales in methane bromination from studying the temperature dependence of the extent of reaction of methane with other bromo- and chloromethanes (Figure 3). As predicted by the data in Table 1 and Scheme 2, reaction of methane with bromine goes to near completion after 60 s at temperatures above 350 °C, while reaction of methane with bromoform requires 100 K higher temperature to go to a similar extent. Activation of methane with dibromomethane at

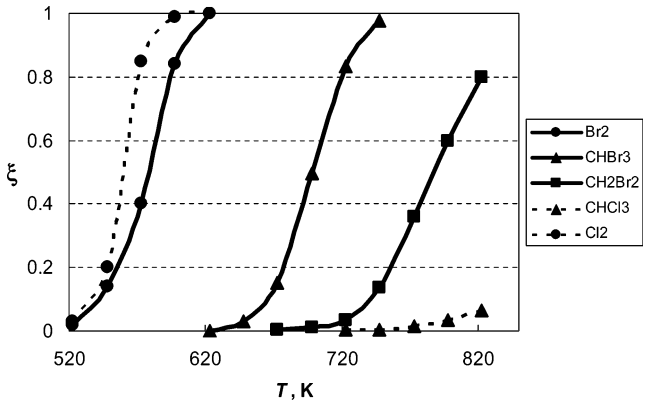

Figure 3. Temperature dependence of extent of reaction (ξ) of methane at 1 atm with bromine and chlorine sources: (●, —) $CH_4 + Br_2 = CH_3Br + HBr$; (●, ---) $CH_4 + Cl_2 = CH_3Cl + HCl$; (▲, —) $CH_4 + CHBr_3 = CH_2Br_2 + CH_3Br$; (■, —) $CH_4 + CH_2Br_2 = 2\ CH_3Br$; (▲, ---) $CH_4 + CHCl_3 = CH_2Cl_2 + CH_3Cl$. For all reactions, methane flow is in at least 10-fold and at most 100-fold stoichiometric excess over the halogen source.

the same reaction time requires an even higher temperature. In a complementary experiment, CH_3Br (250 Torr diluted in N_2) showed only traces (<1%) of disproportionation to methane and dibromomethane (500 °C, 60 s). Loss of CH_2Br_2 to coke and HBr does not compete significantly with these reproportionation reactions under these conditions.

For comparison, reaction of methane with chlorine goes to completion in 60 s at even lower temperature than bromination, but the corresponding reproportionation reaction with chloroform does not occur at significant levels even at 550 °C; instead, other uncharacterized decomposition reactions consume chloroform at this temperature. Dichloromethane is similarly inert under the same conditions.

Summary

We report that methane and bromine react in gas-phase reactors at atmospheric pressure to give a broad range of product distributions that are tunable between kinetic and thermodynamic distributions. Bromination of methane is therefore different from fluorination and chlorination of methane, where the product distribution is kinetically controlled, and the iodination of methane, where the product distribution is thermodynamically controlled. The methyl bromide yield achievable in the second reproportionation phase is twice as high as that predicted on the basis of available thermodynamic data if allowed to react for 60 s at 525 °C. Such unexpectedly high conversion and selectivity of methane to CH_3Br, a potentially universal feedstock, under relatively sustainable reaction conditions is intriguing, while these new experimental product distributions may serve as a baseline for further refinement of C_1 bromocarbon stability constants and thermodynamic properties.[20−22]

Acknowledgment. We thank Professor Eric McFarland, Professor Mike Doherty, and Dr. Mike Weiss for several stimulating discussions.

Appendix 1: Additional Reactions Relevant to CH_xBr_{4-x} Thermal Reproportionation

H-Abstraction Propagations

$$CBr_3 + HBr \leftrightarrow CHBr_3 + Br \quad (15)$$

$$CHBr_2 + HBr \leftrightarrow CH_2Br_2 + Br \quad (16)$$

$$CH_2Br + HBr \leftrightarrow CH_3Br + Br \quad (17)$$

$$CH_3 + HBr \leftrightarrow CH_4 + Br \quad (18)$$

$$CBr_3 + CH_4 \leftrightarrow CHBr_3 + CH_3 \quad (19)$$

$$CBr_3 + CH_3Br \leftrightarrow CHBr_3 + CH_2Br \quad (20)$$

$$CBr_3 + CH_2Br_2 \leftrightarrow CHBr_3 + CH_2Br \quad (21)$$

$$CHBr_2 + CH_4 \leftrightarrow CH_2Br_2 + CH_3 \quad (22)$$

$$CHBr_2 + CH_3Br \leftrightarrow CH_2Br_2 + CH_2Br \quad (23)$$

$$CH_2Br + CH_4 \leftrightarrow CH_3Br + CH_3 \quad (24)$$

Br-Abstraction Propagations

$$H + Br_2 \leftrightarrow HBr + Br \quad (25)$$

$$CBr_3 + HBr \leftrightarrow CBr_4 + H \quad (26)$$

$$CHBr_2 + HBr \leftrightarrow CHBr_3 + H \quad (27)$$

$$CH_2Br + HBr \leftrightarrow CH_2Br_2 + H \quad (28)$$

$$CH_3 + HBr \leftrightarrow CH_3Br + H \quad (29)$$

$$CH_3 + CH_2Br_2 \leftrightarrow CH_3Br + CH_2Br \quad (30)$$

$$CH_3 + CHBr_3 \leftrightarrow CH_3Br + CHBr_2 \quad (31)$$

$$CH_3 + CBr_4 \leftrightarrow CH_3Br + CBr_3 \quad (32)$$

$$CH_2Br + CHBr_3 \leftrightarrow CH_2Br_2 + CHBr_2 \quad (33)$$

$$CH_2Br + CBr_4 \leftrightarrow CH_2Br_2 + CBr_3 \quad (34)$$

$$CHBr_2 + CBr_4 \leftrightarrow CHBr_3 + CBr_3 \quad (35)$$

References and Notes

(1) Anderson, H. C.; Kistiakowsky, G. B.; Van Artsdalen, E. R. *J. Chem. Phys.* **1942**, *10*, 305.
(2) Anderson, H. C.; Kistiakowsky, G. B. *J. Chem. Phys.* **1943**, *11*, 6.
(3) Anderson, H. C.; Van Artsdalen, E. R. *J. Chem. Phys.* **1944**, *12*, 479.
(4) Kistiakowsky, G. B.; Van Artsdalen, E. R. *J. Chem. Phys.* **1944**, *12*, 469.
(5) Golden, D. M.; Benson, S. W. *Chem. Rev.* **1969**, *69*, 125.
(6) Ferguson, K. C.; Okafo, E. N.; Whittle, E. *J. Chem. Soc., Faraday Trans. 1* **1973**, *69*, 295.
(7) Lorkovic, I. M.; Noy, M. L.; Weiss, M.; Sherman, J.; McFarland, E. W.; Stucky, G. D.; Ford, P. C. *Chem. Commun.* **2004**, 566.
(8) Lorkovic, I. M.; Noy, M. L.; Schenck, W. A.; Weiss, M. J.; Sun, S.; Sherman, J. H.; Mcfarland, E. W.; Stucky, G. D.; Ford, P. C. In *American Chemical Society National Meeting, Anaheim, CA, 2004*; Mallinson, R., Ed.; American Chemical Society: Washington, DC, 2004; Vol. 49.
(9) Lorkovic, I. M.; Yilmaz, A.; Yilmaz, G. A.; Zhou, X. P.; Laverman, L. E.; Sun, S.; Schaefer, D. J.; Weiss, M. J.; Noy, M. L.; Cutler, C. I.; Sherman, J.; McFarland, E. W.; Stucky, G. D.; Ford, P. C. *Catal. Today* **2004**, *98*, 317.
(10) Lorkovic, I. M.; Noy, M. L.; Schenck, W. A.; Belon, C.; Weiss, M.; Sun, S.; Sherman, J.; McFarland, E. W.; Stucky, G. D.; Ford, P. C. *Catal. Today* **2004**, *98*, 589.
(11) Sun, S.; Lorkovic, I. M.; Weiss, M.; Sherman, J.; McFarland, E. W.; Ford, P. C.; Stucky, G. D. *Chem. Commun.* **2004**, 2100.
(12) Zhou, X. P.; Lorkovic, I. M.; Stucky, G. D.; Ford, P. C.; Sherman, J.; Grosso, P. U.S. Patent 6,472,572, 2002.
(13) Zhou, X. P.; Yilmaz, A.; Yilmaz, G. A.; Lorkovic, I. M.; Laverman, L. E.; Weiss, M.; Sherman, J.; McFarland, E. W.; Stucky, G. D.; Ford, P. C. *Chem. Commun.* **2003**, 2294.

(14) Yilmaz, A.; Zhou, X. P.; Lorkovic, I. M.; Yilmaz, G. A.; Laverman, L. E.; Weiss, M.; Sun, S.; Schaefer, D. J.; Sherman, J.; McFarland, E. W.; Ford, P. C.; Stucky, G. D. *Microporous Mesoporous Mater.* **2005**, *79*, 205.

(15) Paddison, S. J.; Tschuikow-Roux, E. *J. Phys. Chem. A* **1998**, *102*, 6191.

(16) Weast, R. C., Ed. *CRC Handbook of Chemistry and Physics*, 82nd ed.; CRC: Boca Raton, FL, 2002.

(17) Chase, M. W., Jr., Ed. NIST-JANAF Thermochemical Tables. *J. Phys. Chem. Ref. Data* **1998**, *9*, monograph 9.

(18) Skorobogatov, G. A.; Dymov, B. P.; Tschuikow-Roux, E. *Russ. J. Gen. Chem.* **2003**, *73*, 218.

(19) Dymov, B. P.; Skorobogatov, G. A.; Tschuikow-Roux, E. *Russ. J. Gen. Chem.* **2004**, *74*, 1686.

(20) Oren, M.;. Iron, M. A.; Burcat, A.; Martin, J. M. L. *J. Phys. Chem. A* **2004**, *108*, 7752.

(21) Yao, X.-Q.; Hou, X.-J.; Jiao, H.; Xiang, H.-W.; Li, Y.-W. *J. Phys. Chem. A* **2003**, *107*, 9991.

(22) Marshall, P.; Srinivas, G. N.; Schwartz, M. *J. Phys. Chem. A* **2005**, *109*, 6371.